PLOS ONE

RESEARCH ARTICLE

Correlation coefficient local capping REMD adaptive filtering method for laser interference signal

Junfeng Wu*, Hanyu Chen, Xu Li, Guohua Kang, Yuangang Lu

Key Laboratory of Space Photoelectric Detection and Perception of Ministry of Industry and Information Technology, The College of Astronautics, Nanjing University of Aeronautics and Astronautics, Nanjing, China

* awublack@126.com

OPEN ACCESS

Citation: Wu J, Chen H, Li X, Kang G, Lu Y (2022) Correlation coefficient local capping REMD adaptive filtering method for laser interference signal. PLoS ONE 17(1): e0261875. https://doi.org/10.1371/journal.pone.0261875

Editor: Felix Albu, Valahia University of Targoviste: Universitatea Valahia din Targoviste, ROMANIA

Received: August 21, 2021

Accepted: December 10, 2021

Published: January 21, 2022

Data Availability Statement: The data underlying the results presented in the study are available from (https://github.com/awublack/local-capping-REMD).

Funding: Funding:Supported by the Open Project Program of Wuhan National Laboratory for Optoelectronics.NO. 2019WNLOKF011;National Natural Science Foundation of China under Grant 62175105 and 61875086;Jiang Su province innovative and entrepreneurial talent project. NO - Include this sentence at the end of your statement: The funders had no role in study design, data

Abstract

Considering the issue of noise reduction associated with Laser Doppler Interference (LDI) signal, the paper presented a correlation coefficient local capping robust empirical mode decomposition (REMD) filter algorithm for LDI laser sensor that enables more robust reconstruction of the displacement information from an LDI signal. The performance of the algorithm is studied, and it is shown that the algorithm is capable of removing high-frequency noise. Useful information can be extracted more easily by this method, and the Hilbert phase unwrapping displacement reconstructions method based on this algorithm has been experimentally validated. The experimental results show that the proposed method can improve the frequency separation performance in experiments, and is robust against noise interference.

1. Introduction

Empirical mode decomposition (EMD) is a useful tool for decomposing signals into intrinsic mode functions (IMF). EMD, as the first portion of the Hilbert-Huang transform (HHT) introduced by Huang et al. in 1998, is used in analyzing non-linear and non-stationary time series data [1]. These IMF represent the data using oscillating waves with local zero mean. In some sense, the decomposition can be compared with a time-varying filter [2]. Signals are decomposed using band-limited filters with bandwidths that vary in time. The main advantage of EMD compared to other time-frequency tools is that it does not use any predetermined filters or transforms [3]. Hence, the analysis is adaptive in contrast to traditional methods such as wavelets where the basic functions are fixed and Low-pass filtering, which require a priori information of a signal's frequency characteristics to choose appropriate cutoff frequency [4, 5]. It is therefore a self-contained method that preserves the physical properties in the separate IMFs, explaining why it has been successfully applied in many engineering fields [6–16].

This method has many advantages, but it also has disadvantages From the signal decomposition side, end effects and mode mixing happen and are very common in EMD, and it is very difficult to avoid them [17]. From the signal demodulation side, it has negative frequency problem [18]. The sifting iterations number is directly determined by sifting stopping criterion

collection and analysis, decision to publish, or preparation of the manuscript.

Competing interests: NO authors have competing interests Enter: The authors have declared that no competing interests exist.

(SSC), and it is crucial to the EMD performance. A number of criteria have been proposed. Flandrin et al. proposed the predefined value criterion for the EMD [19]. Another criterion is Cauchy type standard deviation (SD) criteria proposed by Huang et al. [1998]. The criterion can be implemented by limiting the size of the SD by twice sifting the results as defined below:

$$SD = \sum_{t=0}^{T} \frac{[h_{k-1}(t) - h_k(t)]^2}{h_{k-1}^2(t)} \tag{1}$$

A typical value is between 0.2 and 0.3. When the computed SD value lies in the specified range, the sifting process is automatically stopped. These kinds of methods are termed as hard SSC in [20]. The hard criteria requires prior knowledge of the threshold, thus, cannot adapt to signals. A soft sifting stopping criterion is proposed, and it can select the optimal iteration number. This method use mean square (RMS) to define the overall energy of this target signal and Excess Kurtosis (EK) indicator which is the Kurtosis value minus 3 to evaluate the peakedness of one signal. The soft SSC can suppress its mode mixing problem [21]. This adaptive mechanism could stop the sifting process based on the value of the objective function and better performance can be achieved. We will use this robust soft sifting stopping criterion (REMD).

EMD methods combined with correlation coefficient consideration have been studied. EMD based Time Dependent Intrinsic Correlation (TDIC) analysis is applied to consider the correlation between two nonstationary time series [22]. The correlation coefficient between these IMFs was estimated. Rodo and Rodriguez-Aria developed the scale-dependent correlation technique [23]. Although these methods detect the correlation between two nonstationary signals by computing the correlation coefficient in a local sliding window, the main problem is to determine the size of this window. An integrated EMD adaptive threshold denoising method was proposed, and it was showed that a larger correlation coefficient can be offered [24]. A method called center frequency statistical analysis (CFSA) was proposed to determine the number of intrinsic mode function [25]. Compared with maximum center frequency observation (MCFO), correlation coefficient (CC), and normalized mutual information (NMI) methods, CFSA is more robust and accurate. Signal detection based on complete ensemble empirical mode decomposition with adaptive noise and approximate entropy was proposed [26], real IMFs similar to the original signal were selected as final parts through a certain threshold. The problem is that some high-frequency noise signal still has a certain CC value. It is not easy to get focal and informative data, which is happened to be the challenging part of denoising data processing.

Considering these challenges, this paper proposes correlation coefficient local capping with intrinsic mode function (IMF) of empirical mode decomposition (EMD), which over advantage fixed correlation coefficient threshold methods. In this way, it enables reconstructing the signal with more physical relationships. Extensive experiments are conducted to validate the proposed method.

In this paper, we combine REMD with adaptive signal selection by correlation coefficient local capping. The contributions of this paper are summarized as follows:

1. we exploit the characteristics of the correlation coefficient between the empirical modes from the EMD and the original signal to study a new approach to denoising signals.
2. This paper adopts a robust implementation of the soft SSC into sifting process of EMD, and this idea can realize the adaptivity of a sifting process.
3. This paper explores a potential application of REMD to laser interference signal, and displacement is demodulated from the reconstructing signal.

The rest of this paper is organized as follows. A flowchart for the correlation coefficient local capping REMD denoising is provided in section 2. In Section 3, validation of the proposed method is carried out on laser interference signal, and shows a potential ability to demodulation of the laser Doppler interference signal. Finally, Section 4 provides the conclusions of this study.

2. Proposed method local capping REMD

Correlation coefficient local capping REMD is implemented as following steps:

1. For any given data x(n), Initialize the algorithm: $j = 1$, initialize residue $r_0(t) = x(n)$.
2. Identify all the local maxima and minima of $r_{j-1}(n)$.
3. Compute the upper envelope $U_j(n)$ and lower envelope $L_j(n)$ by cubic spline interpolation of local maxima and minima, respectively.
4. Compute the mean of the envelope as $m_j(n) = \frac{(U_j(n)+L_j(n))}{2}$.
5. Take the difference between the data and the mean as the proto-IMF: compute the *jth* component $h_j(n) = r_{j-1}(n) - m_j(n)$.
6. $h_j(n)$ is processed as $r_{j-1}(t)$. Let $h_{j0} = h_j(n)$ and $m_{j,k}(n)$, $k = 0,1\ldots$ be the mean envelope of $h_{jk}(n)$, then compute $h_{jk}(n) = h_{jk-1}(n) - m_{jk-1}(n)$ until the soft stop criterion is satisfied. The stop criterion used here is described as below:

   Define the objective function

$$f_{jk} = RMS_{jk} + |EK_{jk}| \tag{2}$$

$$RMS_{jk} = \sqrt{\frac{1}{N_s}\sum_{n=1}^{N_s}(m_{jk}[n])^2} \tag{3}$$

$$EK_{jk} = \frac{\frac{1}{N_s}\sum_{n=1}^{N_s}(m_{jk}[n] - \overline{m}_j)^4}{(\frac{1}{N_s}\sum_{n=1}^{N_s}(m_{jk}[n] - \overline{m}_j,)^2)^2} - 3 \tag{4}$$

Where $\overline{m}_j$ is the mean of $m_{jk}[n]$. If it meets that: (1) the number of zero points (N_{zp}) and extremal points (N_{ep}) is equal, or the difference between them is less than one; and (2) $f_{k-2} < f_{k-1}$ and $f_{k-1} < f_k$ the sifting process stops and returns the $(k-2)th$ decomposition results. If not, the sifting process does not stop until the number of iterations reaches the maximum iteration number.

7. Compute the *jth* IMF as $IMF_j(t) = h_{j,k}(n)$.
8. Update the residue $r_j(n) = r_{j-1}(n) - IMF_j(n)$.
9. Increase the sifting index j and repeat steps 2 to 8. The signal reconstruction process $x(n)$, which involves combining the IMFs formed from the EMD and the residual

$$x(n) = \sum_{j=1}^{N} IMF_j(n) + r_N(n) \tag{5}$$

10. Compute the correlation coefficients between the input simulation signal and the generated intrinsic mode $Correlation(x(n), IMF_j)$, $j = 1,2,\ldots N$, N is the number of IMFs. The operator $Correlation()$ is defined as:

$$Correlation(X, Y) = r_{XY} = \frac{Cov_{XY}}{S_X S_Y} = \frac{\frac{\sum (X - \overline{X})(Y - \overline{Y})}{(N-1)}}{S_X S_Y} \tag{6}$$

Where

$$S_X = \sqrt{\frac{\sum (X - \overline{X})^2}{N - 1}} \tag{7}$$

$$S_Y = \sqrt{\frac{\sum (Y - \overline{Y})^2}{N - 1}} \tag{8}$$

and based on selected maximum correlation coefficients, we determine the useful IMFs and discard the noisy mode functions (IMFs). Here we reconstruct the signal as

$$\hat{x}(n) = \sum_{j=k+1}^{m-1} IMF_j(n) \tag{9}$$

Here, k and m are index numbers of local minimum and maximum of correlation coefficient respectively centered on the extreme value of the correlation coefficient, and this is just like capping on the extreme. We consider that the maximum correlation coefficient has the maximum correlation with the original signal, and the surrounding adjacent decompositions have a higher dependence on the original signal.

11. Demodulate displacement from the denoising signal.

$$Displacement = unwrap(Arctan(\theta(n))) \frac{\lambda}{4\pi} \tag{10}$$

$$\theta(n) = \arctan \frac{Y(n)}{\hat{x}(n)} \tag{11}$$

$$Y(\mathrm{n}) = Hilbert[\hat{x}(n)] = \frac{1}{\pi} \int_{-\infty}^{+\infty} \frac{\hat{x}(\tau)}{n - \tau} d\tau \tag{12}$$

Where λ is the wavelength of the laser diode. Unwrap is the function for unwrapping the phase angle. This function corrects the radian phase angles by adding multiples of ±2π when absolute jumps between consecutive phase angle are greater than or equal to the jump tolerance of π radians. Arctan is the inverse tangent.

As shown in the flowchart in Fig 1, the displacement is calculated as follows: target signal → REMD → local capping → reconstruction noise-free signal → Hilbert signal → Arctan signal → unwrapping transform → get displacement.

3. Experiment

The validation experiment is carried out according to the following steps. Firstly, the grating is placed on the guide rail driven by the stepping motor. Place a laser interferometer next to it, and scheme of the experimental setup is in the Fig 2. The signal measured by the

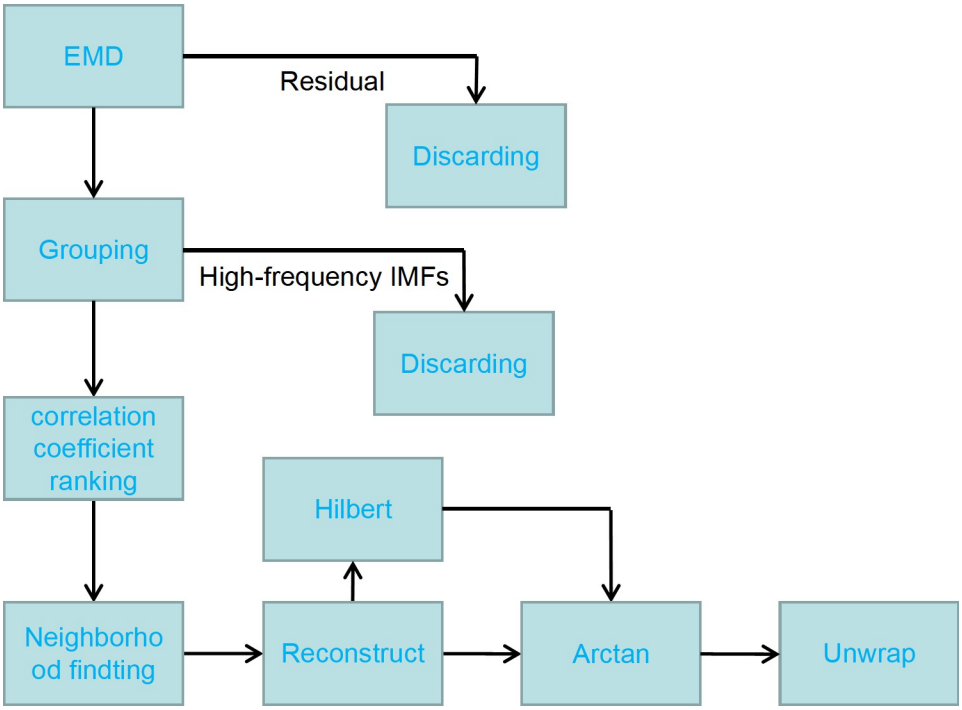

Fig 1. Flowchart of local capping REMD filter.

https://doi.org/10.1371/journal.pone.0261875.g001

interferometer is the input signal. Because the laser of the interferometer has non single-mode characteristics, there will be high-frequency interference signals in the measured signals. The motion of the stepper motor has low-frequency characteristics, resulting in the Doppler effect and Doppler frequency shift.

The method mentioned above is applied to this signal as seen in Fig 3 to extract the displacement signal. Remove the noise signal, and then further demodulate the displacement.

Firstly, the continuous wavelet transform (CWT) based on Morse wavelet is used to analyze signals jointly in time and frequency. It can localize these transients in addition to characterizing oscillatory components in the signal. A signal about 1000-Hz occurs from 14 milliseconds to 16 milliseconds with the maxima magnitude from the global views, as seen in Fig 4. Additionally, there are two transients at 3.5 and 8 milliseconds, and the whole signal is corrupted by noise.

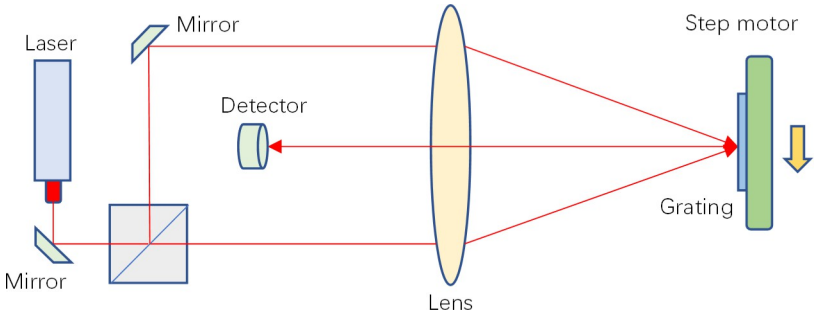

Fig 2. Scheme of the experimental setup.

https://doi.org/10.1371/journal.pone.0261875.g002

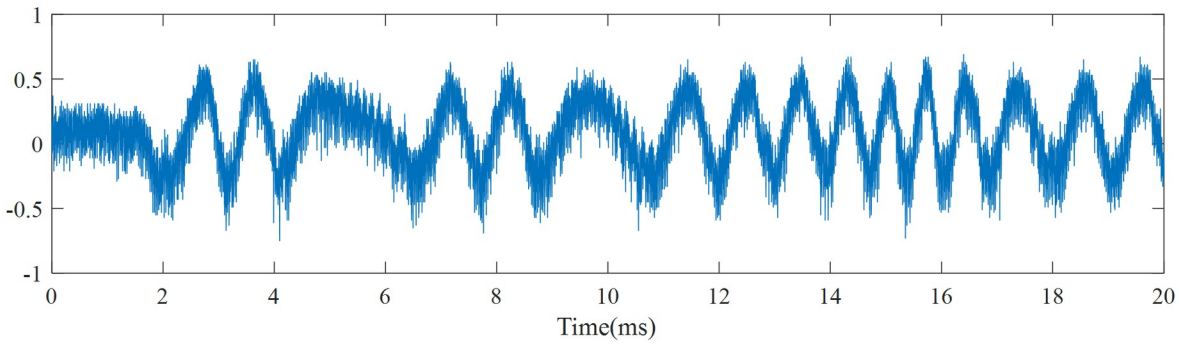

Fig 3. Waveforms of the laser interference signal.

https://doi.org/10.1371/journal.pone.0261875.g003

Then we REMD decompose the input signal, as seen in Fig 5. Through REMD decomposition, nine components and one residue can be obtained. It can be seen that the components of the first five groups are all composed of high-frequency signals. The last four components are composed of low frequencies, and the seventh group has the highest shape similarity with the original signal. In the following calculation, we will use the correlation coefficient to calculate the correlation coefficient between each group and the original signal. It can be seen that the similarity of the shape is also reflected in the size of the correlation coefficient.

In Fig 6 we put all the components into one picture, which can more clearly compare the differences in frequency and amplitude between them. You can see that the seventh group of signals is highlighted in many components

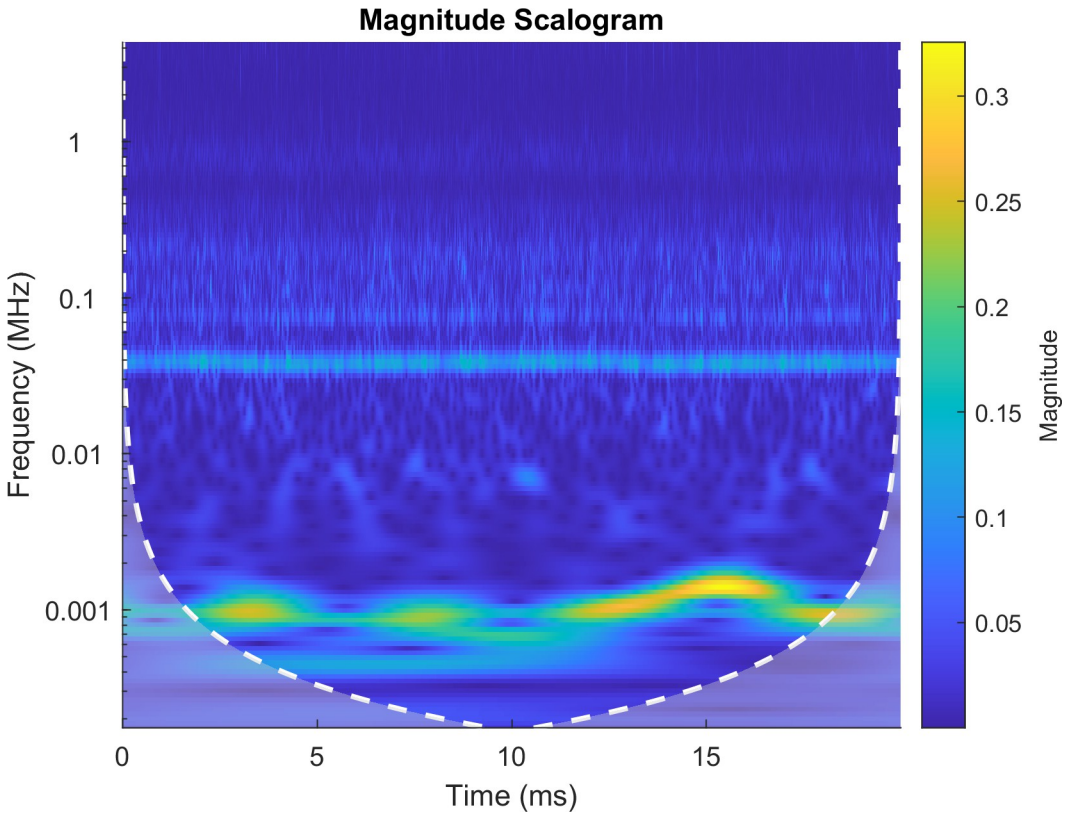

Fig 4. CWT of the input signal.

https://doi.org/10.1371/journal.pone.0261875.g004

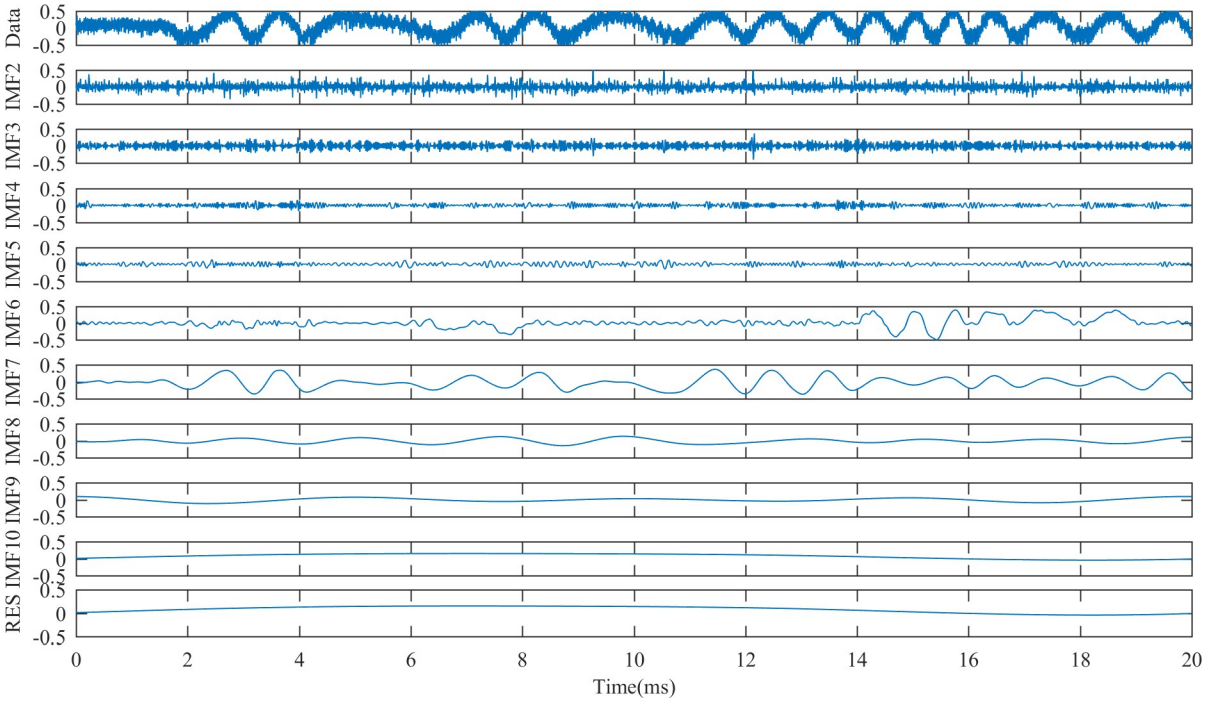

Fig 5. REMD of the input signal.

https://doi.org/10.1371/journal.pone.0261875.g005

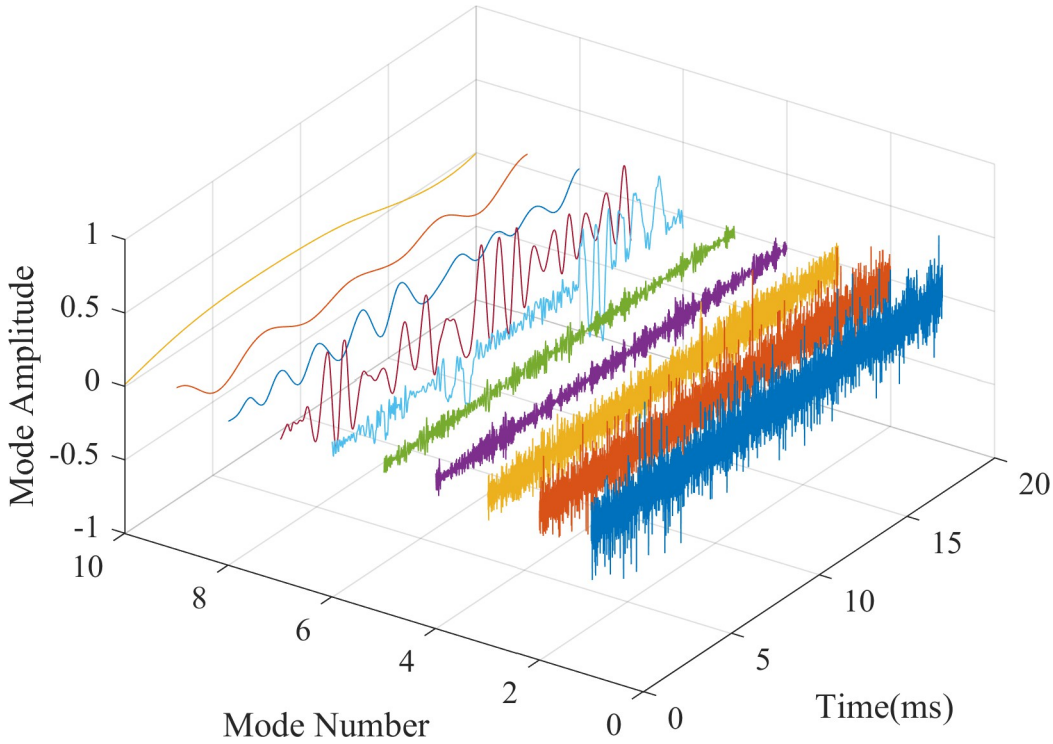

Fig 6. Comparison of IMFs and residual of REMD.

https://doi.org/10.1371/journal.pone.0261875.g006

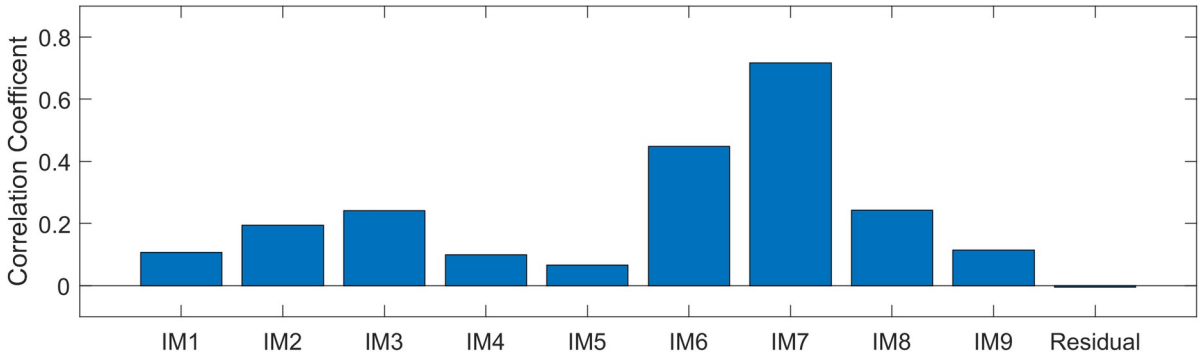

Fig 7. The correlation coefficient of IMFs and residual.

https://doi.org/10.1371/journal.pone.0261875.g007

The maximum correlation coefficient corresponds to the optimal value of the shape parameter, and here the maximum correlation coefficient is finally taken as the similarity score between IMFs and the original signal. Fig 7 below shows that the correlation coefficient between IMFs and the original signal. The IMF7 has the maximum correlation coefficient. It is a useful signal extraction for reconstruction. Take the IMF7 decomposition as the center and recombine the surrounding adjacent decompositions IMF6 and IMF8, which have a higher dependence on the original signal.

Hilbert spectrum is a time spectrum, which can be compared with the spectrum of continuous wavelet transform and short-time Fourier transform, which are also time-frequency analysis methods. This spectrum reflects the change of signal frequency components over time and is an important means to make non-stationary signals. Hilbert spectrum is made for IMF7, and the following results are obtained. With the gradual intensification, the amplitude of the Hilbert spectrum increases in the range of 800 ~ 1200Hz. The **hilbert spectrum of IMF7** is shown in Fig 8.

The corresponding decomposition and reconstruction processes are shown in Fig 9. Firstly, REMD decomposition is carried out. The REMD decomposition signal is composed of high-frequency signal and low-frequency signal. High-frequency signals are mostly noise signals deviate from the maximum correlation coefficient. And how to judge which part is a useful signal. It can be done by the correlation coefficient local capping between the obtained decomposed signal and the original signal. The position with the largest correlation coefficient is the most useful information. Due to the continuity of Doppler signal, the component adjacent to the maximum correlation coefficient is more important. By recombining these signals together, useful information with a high correlation with the doppler signal will can be obtained.

The denoised signal and the original signal are shown in Fig 10. It can be seen that the high-frequency burring signal has been separated from the original signal. The denoised signal can better extract the relevant information in the original signal. Discrete wavelet decomposition could be used in this case, and the main difference is that there is no need to choose which wavelet to use in this method.

The displacement signal can be obtained by solving the interference signal. The specific solution method is as follows. Firstly, the analytical signal of the signal is obtained by the Hilbert transform. The corresponding signal orthogonal to the original signal is obtained. This pair of signals is solved orthogonally. That is, arctangent transformation is used. The corresponding phase is extracted by arctangent transformation. Unwrap this phase item. Thus, the corresponding displacement is obtained. The displacement results are shown in

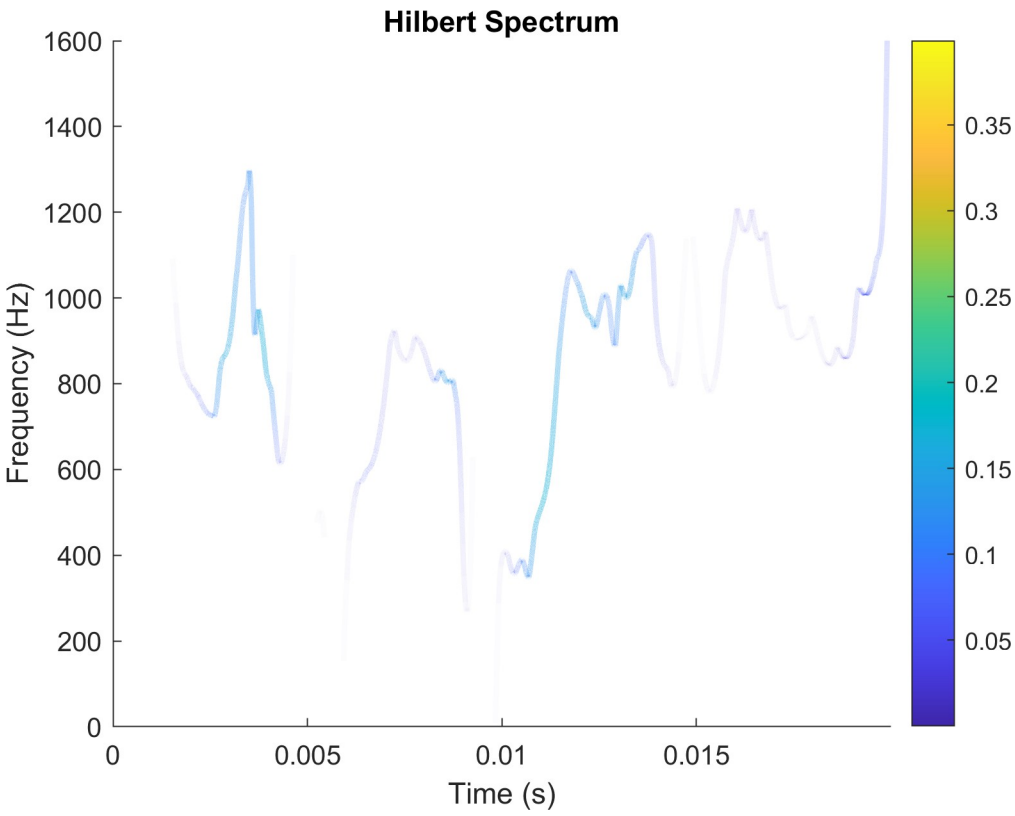

Fig 8. Hilbert spectrum of IMF7.

https://doi.org/10.1371/journal.pone.0261875.g008

Fig 11. The running speed of the guide rail carried by the stepper motor is set to 2.5 millimeter in per second, and the calculated data shown that the whole displacement is 50 micrometers within 20 milliseconds running time, and this result is in good agreement with the experimental setting.

4. Conclusion

The noise reduction process is completed using the correlation coefficient local capping REMD adaptive filter technique. There are three advantages:

1. IMFs decomposed by REMD contain high-frequency signals. These high-frequency signals which are deviate from the maximum correlation coefficients are discarded from the original signal.
2. With the highest correlation coefficient IMF and its local capping adjacent IMFs can be superimposed as reconstructed useful signals, which will get better analysis results, and extracts the low-frequency interference components in the signal.

This method is similar to the EWT method. The EWT method is divided into different frequency bands in the frequency domain. This method selects the point with the highest correlation coefficient as the center point of the useful signal according to the maxima distribution of the correlation coefficient, and expands it in a certain related field to obtain the useful combination of signals. Separate and remove the noise signal with high frequency. A correlation coefficient criterion for extraction useful intrinsic mode function (IMF) is proposed. This

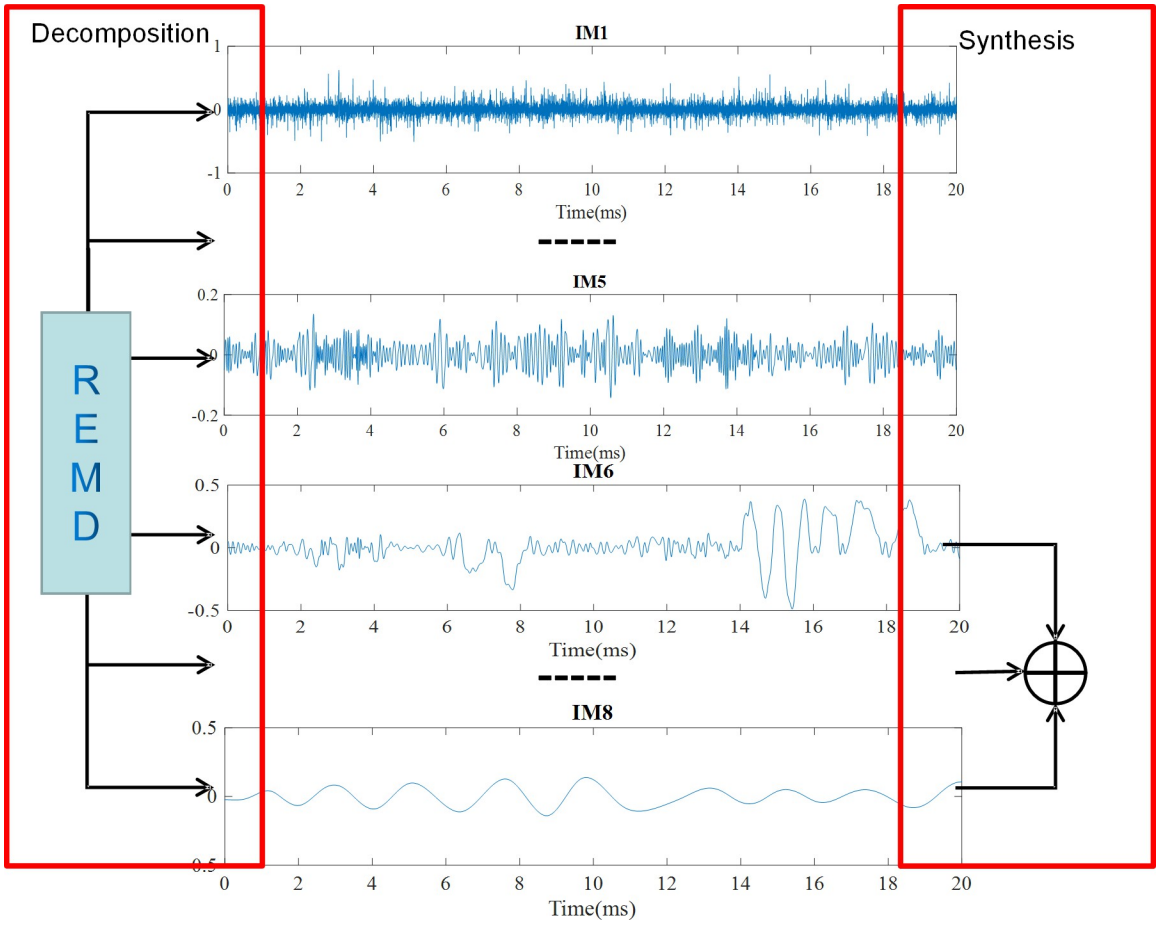

Fig 9. Decomposition and reconstruction process.

https://doi.org/10.1371/journal.pone.0261875.g009

method is fully adaptive and suitable for the analysis of laser interference signals, and the code is freely available as open source on GitHub (https://github.com/awublack/local-capping-REMD).

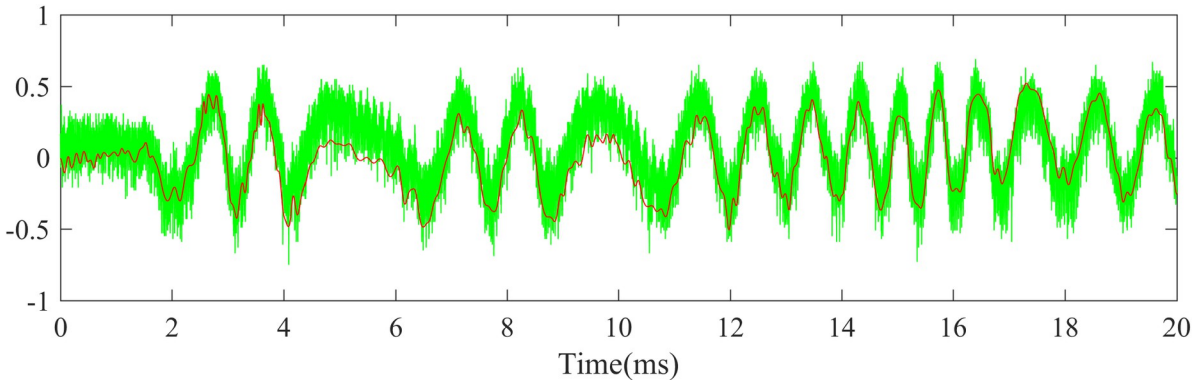

Fig 10. Comparison of denoised signal and the original signal.

https://doi.org/10.1371/journal.pone.0261875.g010

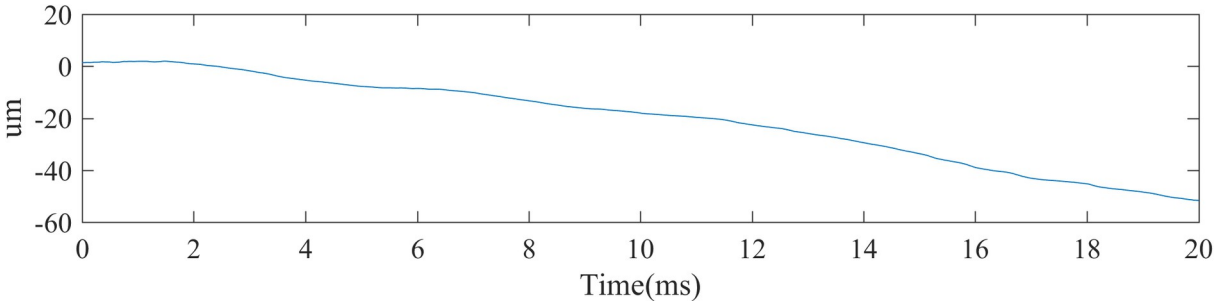

Fig 11. Displacement signal demodulated from noise-free signal.

https://doi.org/10.1371/journal.pone.0261875.g011

Author Contributions

Funding acquisition: Guohua Kang.

Investigation: Guohua Kang, Yuangang Lu.

Methodology: Yuangang Lu.

Software: Junfeng Wu.

Visualization: Yuangang Lu.

Writing – original draft: Junfeng Wu.

Writing – review & editing: Hanyu Chen, Xu Li, Guohua Kang.

References

1. Huang NE, Shen Z, Long SR, Wu MC, Shih HH, Zheng Q, et al. The empirical mode decomposition and the Hilbert spectrum for nonlinear and non-stationary time series analysis. Proceedings of the Royal Society of London Series A: Mathematical, Physical and Engineering Sciences. 1998; 454(1971):903–95. https://doi.org/10.1098/rspa.1998.0193 PMID: 26953177
2. Assous S, Humeau A, huillier JL, editors. Empirical Mode Decomposition Applied to Laser Doppler Flowmetry Signals: Diagnosis Approach. 2005 IEEE Engineering in Medicine and Biology 27th Annual Conference; 2005 17–18 Jan. 2006.
3. Wang Q, Jiang Q. Simulation of Matched Field Processing Localization Based on Empirical Mode Decomposition and Karhunen-Loève Expansion in Underwater Waveguide Environment. EURASIP Journal on Advances in Signal Processing. 2010; 2010(1):483524. https://doi.org/10.1155/2010/483524
4. Liu S, Gao RX, John D, Staudenmayer J, Freedson P. Tissue artifact removal from respiratory signals based on empirical mode decomposition. Ann Biomed Eng. 2013; 41(5):1003–15. Epub 2013/01/17. https://doi.org/10.1007/s10439-013-0742-5 PMID: 23325303.
5. Zhang J, Soangra R, E. Lockhart T. A Comparison of Denoising Methods in Onset Determination in Medial Gastrocnemius Muscle Activations during Stance. Sci. 2020; 2(3). https://doi.org/10.3390/sci2030053
6. Cheng Y, Wang Z, Chen B, Zhang W, Huang G. An improved complementary ensemble empirical mode decomposition with adaptive noise and its application to rolling element bearing fault diagnosis. ISA Transactions. 2019; 91:218–34. https://doi.org/10.1016/j.isatra.2019.01.038 PMID: 30738582
7. Nguyen H-P, Baraldi P, Zio E. Ensemble empirical mode decomposition and long short-term memory neural network for multi-step predictions of time series signals in nuclear power plants. Applied Energy. 2021; 283:116346. https://doi.org/10.1016/j.apenergy.2020.116346.
8. Huo W, Wang C, Da F. Fast fringe enhancement by improved bidimensional sinusoids-assisted empirical mode decomposition. Optik. 2021:167834. https://doi.org/10.1016/j.ijleo.2021.167834.
9. Dong S, Zhou Y, Chen T, Li S, Gao Q, Ran B. An integrated Empirical Mode Decomposition and Butterworth filter based vehicle trajectory reconstruction method. Physica A: Statistical Mechanics and its Applications. 2021; 583:126295. https://doi.org/10.1016/j.physa.2021.126295.

10. Ying W, Zheng J, Pan H, Liu Q. Permutation entropy-based improved uniform phase empirical mode decomposition for mechanical fault diagnosis. Digital Signal Processing. 2021; 117:103167. https://doi.org/10.1016/j.dsp.2021.103167.

11. Cheng G, Wang X, He Y. Remaining useful life and state of health prediction for lithium batteries based on empirical mode decomposition and a long and short memory neural network. Energy. 2021; 232:121022. https://doi.org/10.1016/j.energy.2021.121022.

12. Shrivastava Y, Singh B. Tool chatter prediction based on empirical mode decomposition and response surface methodology. Measurement. 2021; 173:108585. https://doi.org/10.1016/j.measurement.2020.108585.

13. Yao Z, Wang Z, Liu X, Wang C, Shang Z. An improved low-frequency noise reduction method in shock wave pressure measurement based on mode classification and recursion extraction. ISA Transactions. 2021; 109:315–26. https://doi.org/10.1016/j.isatra.2020.10.022 PMID: 33041011

14. The PONES. Correction: Empirical mode decomposition processing to improve multifocal-visual-evoked-potential signal analysis in multiple sclerosis. PLOS ONE. 2018; 13(5):e0196928. https://doi.org/10.1371/journal.pone.0196928 PMID: 29715325

15. Gao K, Xu X, Li J, Jiao S, Shi N. Application of multi-layer denoising based on ensemble empirical mode decomposition in extraction of fault feature of rotating machinery. PLOS ONE. 2021; 16(7):e0254747. https://doi.org/10.1371/journal.pone.0254747 PMID: 34280237

16. Barnova K, Martinek R, Jaros R, Kahankova R, Matonia A, Jezewski M, et al. A novel algorithm based on ensemble empirical mode decomposition for non-invasive fetal ECG extraction. PLOS ONE. 2021; 16(8):e0256154. https://doi.org/10.1371/journal.pone.0256154 PMID: 34388227

17. Zeiler A, Faltermeier R, Keck IR, Tomé AM, Puntonet CG, Lang EW, editors. Empirical Mode Decomposition—an introduction. The 2010 International Joint Conference on Neural Networks (IJCNN); 2010 18–23 July 2010.

18. Yue S, Wang Y, Wei L, Zhang Z, Wang H. The joint empirical mode decomposition-local mean decomposition method and its application to time series of compressor stall process. Aerospace Science and Technology. 2020; 105:105969. https://doi.org/10.1016/j.ast.2020.105969.

19. Flandrin P, Rilling G, Goncalves P. Empirical mode decomposition as a filter bank. IEEE Signal Processing Letters. 2004; 11(2):112–4. https://doi.org/10.1109/LSP.2003.821662

20. Liu Z, Zuo MJ, Jin Y, Pan D, Qin Y. Improved local mean decomposition for modulation information mining and its application to machinery fault diagnosis. Journal of Sound and Vibration. 2017; 397:266–81. https://doi.org/10.1016/j.jsv.2017.02.055.

21. Liu Z, Peng D, Zuo MJ, Xia J, Qin Y. Improved Hilbert–Huang transform with soft sifting stopping criterion and its application to fault diagnosis of wheelset bearings. ISA Transactions. 2021. https://doi.org/10.1016/j.isatra.2021.07.011 PMID: 34281714

22. Ismail DKB, Lazure P, Puillat I. Advanced Spectral Analysis and Cross Correlation Based on the Empirical Mode Decomposition: Application to the Environmental Time Series. IEEE Geoscience and Remote Sensing Letters. 2015; 12(9):1968–72. https://doi.org/10.1109/LGRS.2015.2441374

23. Rodó X, Rodríguez-Arias M-À. A new method to detect transitory signatures and local time/space variability structures in the climate system: the scale-dependent correlation analysis. Climate Dynamics. 2006; 27(5):441–58. https://doi.org/10.1007/s00382-005-0106-4

24. Zhang M, Wei G. An integrated EMD adaptive threshold denoising method for reduction of noise in ECG. PLOS ONE. 2020; 15(7):e0235330. https://doi.org/10.1371/journal.pone.0235330 PMID: 32667934

25. Wu S, Feng F, Zhu J, Wu C, Zhang G. A Method for Determining Intrinsic Mode Function Number in Variational Mode Decomposition and Its Application to Bearing Vibration Signal Processing. Shock and Vibration. 2020; 2020:8304903. https://doi.org/10.1155/2020/8304903

26. Shang H, Li Y, Xu J, Qi B, Yin J. A Novel Hybrid Approach for Partial Discharge Signal Detection Based on Complete Ensemble Empirical Mode Decomposition with Adaptive Noise and Approximate Entropy. Entropy (Basel, Switzerland). 2020; 22(9). Epub 2020/12/09. https://doi.org/10.3390/e22091039 PMID: 33286808; PubMed Central PMCID: PMC7597099.